

۱ **The antimicrobial and antibiofilm potential of *Citrus aurantium* and *Artemisia***
۲ ***annua* essential oils nanoemulsions**

۳
۴ Mahmoud Osanloo¹, Hiva Alipanah², MohammadArman Hashempour³, Benyamin Motazedian³,
۵ Elham Zarenezhad⁴, Zahra Zahedifard⁵, Abdolmajid Ghasemian^{4*}

- ۶
۷ 1. Department of Medical Nanotechnology, School of Advanced Technologies in Medicine,
۸ Fasa University of Medical Sciences, Fasa, Iran
۹ 2. Department of Physiology, School of Medicine, Fasa University of Medical Sciences,
۱۰ Fasa, Iran
۱۱ 3. Department of Medicine, School of Medicine, Fasa University of Medical Sciences, Fasa,
۱۲ Iran
۱۳ 4. Noncommunicable Diseases Research Center, Fasa University of Medical Sciences, Fasa,
۱۴ Iran
۱۵ 5. Department of Medical Biotechnology, School of Advanced Technologies in Medicine,
۱۶ Fasa University of Medical Sciences, Fasa, Iran
۱۷

۱۸ **Running titles:** Natural nano-antibiotics

۱۹
۲۰ ***Corresponding author:** Abdolmajid Ghasemian, email: majidghasemian86@gmail.com,
۲۱ phone: +98 9106806917, Noncommunicable Diseases Research Center, Fasa University of
۲۲ Medical Sciences, Fasa, Iran, ORCID: <https://orcid.org/0000-0002-1243-6341>

٢٥ **ABSTRACT**

٢٦ Antimicrobial resistance has posed considerable health and economic burdens globally
٢٧ (approximately five million deaths annually), particularly among developing countries. The
٢٨ estimated annual treatment costs in the United States include US\$4.6 billion. Vast antibiotic
٢٩ resistance among Gram-negative and Gram-positive bacterial species has spread from healthcare
٣٠ to the environment, community, and animals. These conditions have limited and sometimes
٣١ failed the infection eradication choices and facilitated the distribution of drug-resistant
٣٢ organisms. The spread of drug-resistant bacterial infections is a huge human health concern,
٣٣ hence seeking novel antibacterial agents is crucial. This study used the nanoemulsions of *Citrus*
٣٤ *aurantium* and *Artemisia annua* essential oils (EOs) as natural antibacterial agents. Gas
٣٥ chromatography mass spectrometry (GC-MS) analysis showed that limonene (31.4%) and
٣٦ artemisia ketone (26.2%) were major components, respectively. After that, their nanoemulsion
٣٧ dosage forms with a mean droplet size of 181 ± 7 and 160 ± 5 and with zeta potential values 3.1
٣٨ ± 0.8 and -4.9 ± 0.5 mV were prepared. Meanwhile, successful loading of the EOs in
٣٩ nanoemulsion was confirmed by Attenuated Total Reflection-Fourier Transform Infrared (ATR-
٤٠ FTIR) analysis. *A. annua* nanoemulsion with 40% antioxidant effect was significantly more
٤١ potent than *C. aurantium* nanoemulsion. Meanwhile, nanoemulsions' antibacterial and
٤٢ antibiofilm activity against clinical and standard strains, *Escherichia coli*, *Staphylococcus*
٤٣ *aureus*, *Pseudomonas aeruginosa*, and *Klebsiella pneumonia*, were investigated. The best
٤٤ efficiency was related to the effect of *C. aurantium* nanoemulsion against *S. aureus*; minimum
٤٥ inhibitory and bactericidal concentrations (respectively MIC and MBC) were 500 and > 2000
٤٦ $\mu\text{g/mL}$. Besides, no biofilm was formed after treatment by both nanoemulsions. Therefore, *C.*

εν *aurantium* and *A. annua* EO nanoemulsions may act as natural antioxidant and antibacterial
ελ agents in complementary medicine.

εϑ **Keywords:** Antibacterial Agents, Essential Oil, Reactive Oxygen Species, Phytochemicals

Preprint

1. Introduction

Vast antibiotic resistance among Gram-negative and Gram-positive bacterial species has spread from healthcare to the environment, community, and animals. These conditions have limited and sometimes failed the infection eradication choices, resulting in the distribution of drug-resistant organisms (1, 2) such as those non-susceptible to last-resort antibiotics of carbapenems and glycopeptides. As alternatives to chemotherapies, natural resources such as essential oils (EOs) have been suitable alternatives (3-5). In addition, nanoformulation of EOs by optimization in particle size, increasing solubility, and improving bioavailability and stability causes medicines to be more permeable into cells, such as bacteria or cancer cells (6-10). The *citrus* genus includes several species of citrons within the family *Rutaceae*, utilized as herbal medicines, fruits, juice, and additives. *Citrus* fruits contain vitamins C and B, minerals, nutrients, and bioactive compounds such as phenolic compounds, volatile oils, and terpenoids. *Citrus aurantium* (*C. aurantium*) L. cultivar has exhibited anti-inflammatory, hypoglycemic, antimicrobial, anticancer, pain-relief, and organ protective effects (11). Although the species has bioactive compounds and biological activities, its pharmacological effects, traditional usage, and exact bioactive compounds have not been uncovered (12). On the other, *C. aurantium* L. dietary supplementation has not exerted side effects (13). Various extracts of *C. aurantium* L. leaves, including aqueous, alcoholic, or chloroform portions, have demonstrated antibacterial effects against various agents (11, 13). In addition, the antimicrobial effects of its EOs have unraveled potential activities against *Agrobacterium tumefaciens*, *Dickeya solani*, and *Erwinia amylovora* (14, 15). *Artemisia annua* grows globally in Europe, Asia and North America with preferred arid and semi-arid climates and provides considerable health benefits such as anticancer and antimicrobial traits. Bioactive compounds of the herb mainly include artemisia ketone, 1,8-

73 cineole, germacrene D, and camphor (16). This study aimed to investigate the antibacterial and
74 antibiofilm effects of nanoemulsions of *A. annua* L. and *C. aurantium*.

75 **2. Materials and Methods**

76 **2.1. Materials**

77 *C. aurantium* and *A. annua* EOs were bought from Iranian companies, Tabib Daru
78 Company and Pharmaceutical Company Essential Oil Dr. Soleimani. Bacterial standard strains
79 included *Escherichia coli* ATCC25922, *Staphylococcus aureus* ATCC25923, *Pseudomonas*
80 *aeruginosa* ATCC 27853, and *Klebsiella pneumonia* ATCC13883 were cultured from bacterial
81 stock preserved at -20 °C in the microbiology laboratory of Fasa University of Medical Sciences,
82 Iran. Moreover, clinical isolates were collected from patients. Mueller Hinton broth, trypticase
83 soy broth, crystal violet, tween 20, and tween 80 were purchased from Merck Chemicals,
84 Germany. The standard analytical solution of Alkanes (C9-C24) was bought from Sigma-Aldrich
85 (USA).

87 **2.2. Chemical composition of EOs**

88 [Gas chromatography mass spectrometry \(GC–MS\)](#) analysis was used for the chemical
89 compositions of the EOs. For this purpose, the gas chromatographic device (Agilent 6890, USA)
90 with HP-5MS silica fused columns coupled to a network mass selective detector (Agilent 5973,
91 USA) was used. The major constituents of EOs were identified by comparing their retention
92 indices to homologous C9-C24 n-alkanes, as described in our previous reports (17, 18).

93 **2.3. Preparation and characterizations of nanoemulsions**

94 *A. annua* EO (0.4% v/v) was mixed with tween 80 (0.5% v/v), and *C. aurantium* (0.4%
95 v/v) was mixed with tween 20 (0.5% v/v), separately, for 3 minutes at room temperature at 2000 rpm.
96 Afterward, distilled water was added drop by drop to reach the final volume of 5 mL, and the

1.97 mixture was stirred for 40 minutes at room temperature at 2000 rpm. The prepared
1.98 nanoemulsions' droplet size and droplet size distribution (SPAN) were measured using a DLS
1.99 (Dynamic Light Scattering, DLS9900, K-ONE, Korea) device. SPAN was calculated using the
2.00 relationship $d_{90}-d_{10}/d_{50}$; in this equation, d is the diameter, 90, 10, and 50 percent of particles
2.01 with a size smaller than the values mentioned. The droplet size below 200 nm and SPAN below
2.02 one were necessary conditions to confirm the appropriate size characteristics. TEM (Transitional
2.03 Electron Microscopy, Philips, TEM, EM 208s, Netherland) was used to confirm the droplet size
2.04 and determine their morphology. ATR-FTIR (Attenuated Total Reflection-Fourier Transform
2.05 Infrared) analysis is used to evaluate the successful loading of the EOs in the nanoemulsion.
2.06 Spectra of the EOs, nanoemulsion (-oil), and nanoemulsion were recorded in $400 - 4000 \text{ cm}^{-1}$
2.07 using a spectrometer (Tensor II model, Bruker Co, Germany). Furthermore, the stability of
2.08 nanoemulsions was investigated. Nanoemulsions were centrifuged at -4 , $+4$, and $+25^{\circ}\text{C}$ (14,000
2.09 g, 30 min) to investigate stability against precipitation. Besides, nanoemulsions were stored at
2.10 $+45^{\circ}\text{C}$ and room temperature for six consecutive intervals of 48 hours for thermal stability
2.11 analysis. Moreover, nanoemulsions were placed at -20°C and room temperature for six
2.12 consecutive 48-hour intervals for cryogenic stability. In addition, nanoemulsions were placed at
2.13 4°C and room temperature for six months for long-term stability analysis. After each test, the
2.14 nanoemulsion was visually checked for sedimentation, creaming, or biphasic.

2.4. Investigation of antioxidant properties of EOs and nanoemulsions

2.16 DPPH (2,2-diphenyl-1-picrylhydrazyl) assay was used to measure antioxidant properties.
2.17 First, serial dilutions of the nanoemulsions (62.5-2000 $\mu\text{g}/\text{mL}$) were prepared in ethanol. Next,
2.18 50 $\mu\text{L}/\text{well}$ of each prepared dilution and 0.2 mM DPPH solution was added to a 96-well plate,
2.19 and it was incubated for 30 minutes away from light at room temperature. Finally, the wells' OD

120 (optical density) was read at 517 nm using a plate reader (Synergy HTX Multi-Model Reader,
121 USA).

122 The antioxidant activity was calculated using $OD_{test}/OD_{control} \times 100$.

123 **2.5. Minimum inhibitory concentration**

124 **Micro-dilution test was implemented.** The range of concentrations of nanoemulsions
125 (250, 500, 1000, 1500 and 2000 $\mu\text{g}/\text{mL}$) was prepared by PBS containing 0.5% DMSO as
126 solvent. Antibacterial effects of EOs and nanoemulsion were investigated using 96-well broth
127 micro-dilution, as described in our previous study (19). Briefly, 40 μL of each was inoculated
128 into wells of 96 well plates containing 50 μL of Mueller Hinton broth. Afterward, 10 μL /well of
129 each bacterial suspension (0.5 McFarland standard turbidity, 1.5×10^8 CFU/mL) was added to
130 each well. The plates were incubated for 24 hours at 37 °C, and then the OD of the wells was
131 read at 630 nm. Bacterial growth was obtained using $OD_{sample}/OD_{control} \times 100$. The minimum
132 inhibitory concentration (MIC) of *A. annua* and *C. aurantium* single and nanoemulsion forms
133 against bacterial strains were determined using concentrations ranging from 250-2000 $\mu\text{g}/\text{mL}$.
134 Moreover, the bacterial suspension equal to 0.5 McFarland standard was prepared. The test was
135 performed the same as that of the broth micro-dilution method.

136 **2.6. Biofilm formation**

137 Anti-biofilm effects of EOs and nanoemulsions were assessed against clinical isolates.
138 biofilm The biofilm formation with and without exposure to the nanoemulsions was performed
139 into 96-well plates using a microtitre tissue plate assay. Briefly, an overnight culture of bacterial
140 strains was obtained into the trypticase soy broth (TSB) medium containing 1% glucose and
141 diluted 1:100. For each bacterial suspension, 20 μL was taken and inoculated into wells
142 containing 180 μL of the TSB medium in triplicate and incubated for 5 hours for exposed (2000

143 $\mu\text{g/mL}$ of each nanoemulsion) group and 24h for the un-exposed group. The un-exposed group
 144 medium was exchanged with each nanoemulsion and incubated for 24 hours. Next, the wells
 145 were washed using double distilled water and fixed using methanol. Then, 0.1% crystal violet or
 146 safranin was added for 15 min. After repeated washing, the absolute ethanol (200 μL) was added
 147 to solubilize bacterial contents and read using the ELISA reader at 490 nm. The biofilm
 148 formation levels (strong, moderate, weak, or non-adherence) were calculated using Table 1. This
 149 study compared biofilm formation levels among groups, including the control (unexposed) and
 150 *A. annua* and *C. aurantium* EOs nanoemulsion-treated groups.

151 **Table1.** The calculation of biofilm formation levels

Biofilm formation ability	Calculation of cut-off level	OD calculated results	Reference
Strong	$\text{OD} > \text{ODc} \times 4$	$0.33296 > \text{OD}$	(20, 21)
Moderate	$\text{ODc} \times 2 \leq \text{OD} < \text{ODc} \times 4$	$0.16648 \leq \text{OD} < 0.33296$	
Weak	$\text{ODc} \leq \text{OD} < 2 \times \text{ODc}$	$0.083324 \leq \text{OD} < 0.16648$	
No binding	$\text{OD} \leq \text{ODc}$	$0.08324 \leq \text{OD}$	

152 OD: optical density, ODc: mean OD of control wells

153 2.7.Data analysis

154 All experiments were done in triplicates. The data was analyzed using the SPSS version,
 155 from which Chi-Square and analysis of variance (ANOVA) tests were applied to determine
 156 differences at a *p*-value cut-off of 0.05.

157 3. Results

158 The main components of the *C. aurantium* were limonene (31.4%), sabinene (15.6%), γ -
 159 terpinene (6.0%), linalool (5.6%) and cis-nerolidol (5.1%) (Table 2). As well as the main
 160 components of the *A. annua* were artemisia ketone (26.2%), camphor (19.2%), 1,8-cineole
 161 (12.3%), *trans*-caryophyllene (4.5%), and camphene (4.4%) (Table 2).

Table 2. Identified compounds in the EOs using GC-MS analysis

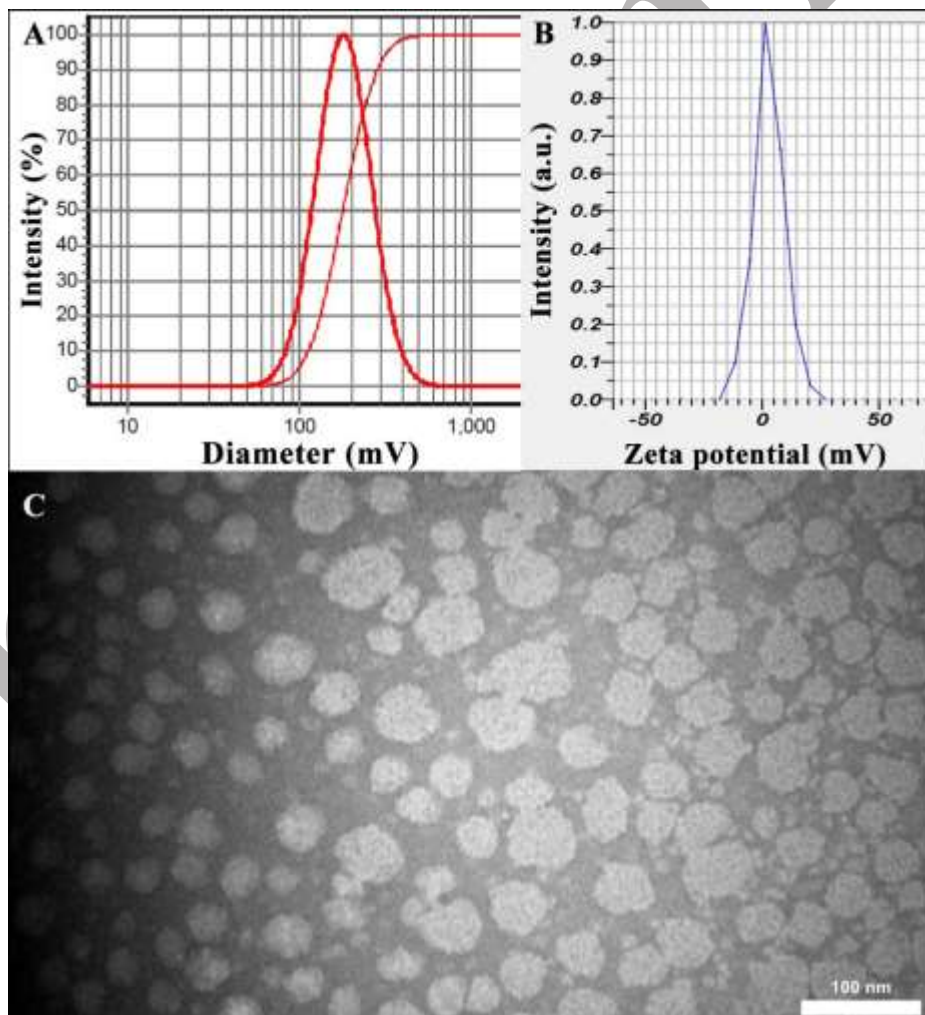
Retention Time (min)	Compound	<i>C. aurantium</i>		<i>A. annua</i>		Retention Index
		Area	%	Area	%	
9.46	α -pinene	58484827	1.7	122296938	4.1	932
10.06	camphene	--	--	132788539	4.4	954
11.14	sabinene	542668432	15.6	44039171	1.5	975
11.24	β -pinene	43301938	1.2	29556997	1.0	979
11.96	β -myrcene	108784770	3.1	29379228	1.0	988
12.50	Yomogi alcohol	--	--	41103264	1.4	999
13.08	α -terpinene	59177141	1.7	--	--	1014
13.81	1,8-cineole	--	--	368453758	12.3	1026
13.89	limonene	1088445097	31.4	--	--	1029
14.67	<i>cis</i> -ocimene	162728160	4.7	--	--	1037
15.13	γ -terpinene	207125216	6.0	--	--	1054
15.48	artemisia ketone	--	--	784989266	26.2	1062
16.31	artemisia alcohol	--	--	33487881	1.1	1083
17.16	linalool	192637034	5.6	--	--	1095
19.22	camphor	--	--	576552736	19.2	1146
20.12	borneol	--	--	28483988	1.0	1169
20.63	4-terpineol	66692764	1.9	33586786	1.1	1177
23.55	cuminic aldehyde	128003231	3.7	--	--	1239
29.38	α -copaene	--	--	47639328	1.6	1376
31.26	<i>trans</i> -caryophyllene	--	--	136219018	4.5	1419
33.78	germacrene D	--	--	84811438	2.8	1481
33.99	β -selinene	--	--	90133377	3.0	1490
37.11	<i>cis</i> -nerolidol	178234586	5.1	--	--	1532
37.76	caryophyllene oxide	--	--	35663606	1.2	1583
42.89	<i>cis</i> -farnesol	34776356	1.0	--	--	1698

163

164 3.1. TEM analysis of *C. aurantium* and *A. annua* EO nanoemulsions

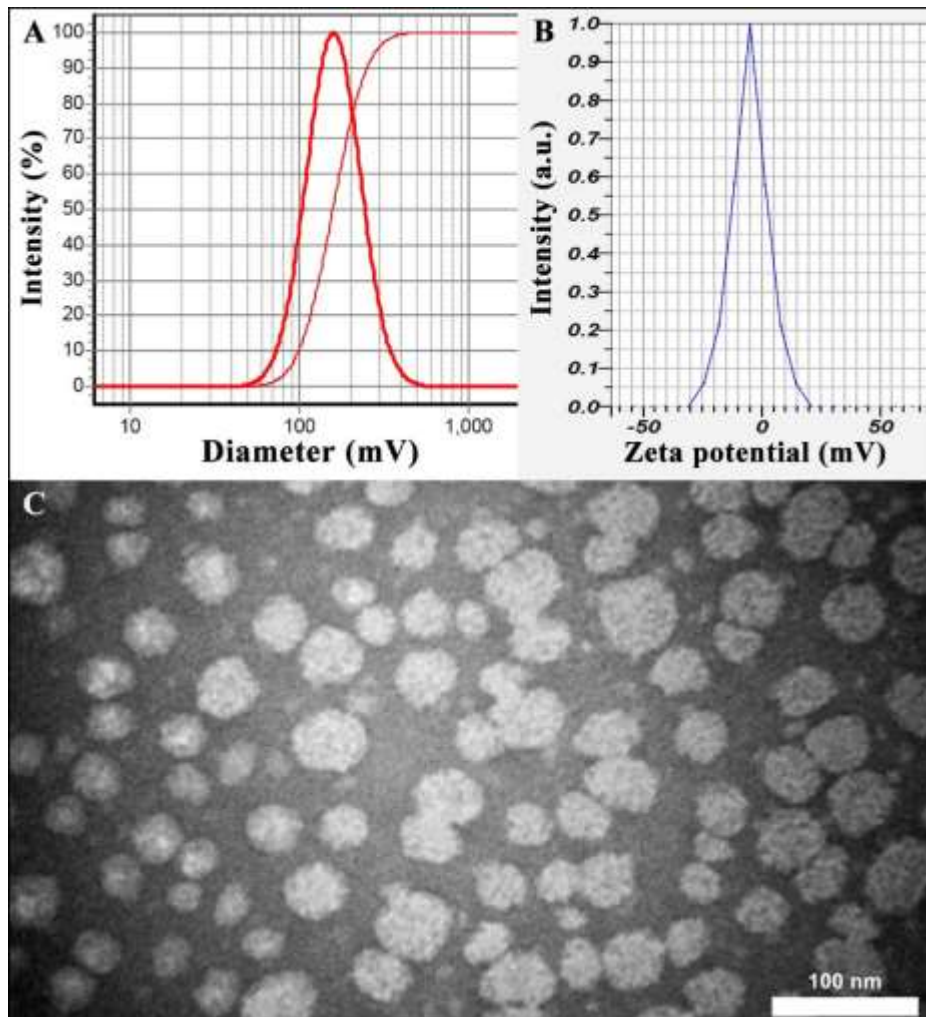
165 The mean droplet diameter and zeta potential of *C. aurantium* nanoemulsion were $181 \pm$
 166 7 nm and 3.1 ± 0.8 mV, respectively (**Figure 1 A & B**). The *A. annua* nanoemulsions showed
 167 droplet diameter at 160 ± 5 nm and zeta potential values -4.9 ± 0.5 mV (**Figure 2 A & B**). The
 168 TEM analysis (**Figures 1C and 2C**) revealed that both nanoemulsions were spherical, size < 100
 169 nm.

170 Furthermore, the stability of nanoemulsions was investigated. Nanoemulsions were
171 centrifuged at -4 , $+4$, and $+25^{\circ}\text{C}$ (14,000 g, 30 min); no sedimentation or bi-phasic was
172 observed. Besides, nanoemulsions were stored at $+45^{\circ}\text{C}$ and room temperature for six
173 consecutive intervals of 48 hours for thermal stability analysis; no sedimentation or bi-phasic
174 was observed. Moreover, nanoemulsions were placed at -20°C and room temperature for six
175 consecutive 48-hour intervals for cryogenic stability; no sedimentation or bi-phasic was
176 observed. In addition, nanoemulsions were placed at 4 and room temperature for six months for
177 long-term stability analysis; no sedimentation or bi-phasic was observed.



178

179 **Figure 1.** Characterization of *C. aurantium* EO nanoemulsion, A: DLS profile, B: zeta potential
180 profile, and C: TEM image



181
182 **Figure 2.** Characterization of *A. annua* EO nanoemulsion, A: DLS profile, B: zeta potential
183 profile, and C: TEM image

184 3.2. ATR-FTIR analysis of *C. aurantium* and *A. annua* nanoemulsions

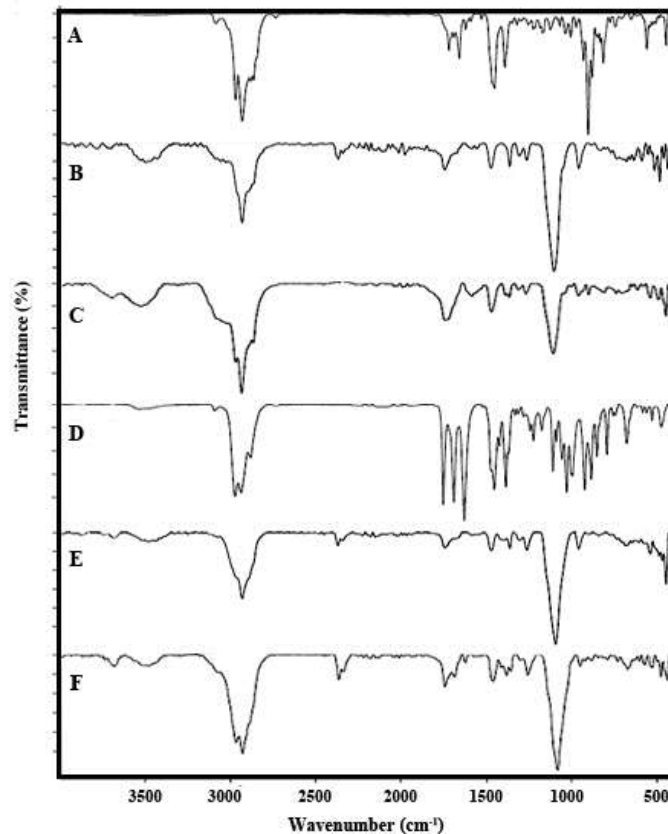
185 ATR-FTIR analysis confirmed EO loading in nanoemulsion (**Figure 3**). The spectra of *C.*
186 *aurantium* EO displayed in Figure 3A, broadband at 3469 cm^{-1} can be related to stretching
187 vibration of the hydroxyl group due to hydrogen bonding in alcoholic and phenolic bioactive
188 compounds in EO, spectra at 3076 cm^{-1} can be corresponded to stretching vibration of CH in sp^2
189 groups and the bands at 2961 , 2923 and, 2872 cm^{-1} can be attributed to stretching vibration of

190 CH in sp^3 groups, the band at 1706 and 1676 cm^{-1} can be related to stretching vibration of
191 carbonyl groups. Bands at 1108 and 1052 cm^{-1} showed stretching vibration of C-O groups. The
192 peak at 989 cm^{-1} is related to C-H bending absorption, and the strong peak at 758 cm^{-1} is
193 allocated to benzene rings C-H vibration absorption. A peak at 689 cm^{-1} is attributed to the
194 vibration absorption of alkenes. The spectrum of nanoemulsion without *C. aurantium* EO
195 displayed in Figure 3B, the broad peak at about 3493 cm^{-1} can be attributed to OH stretching
196 vibration due to hydrogen bonding between water and tween 20. Spectra at 2924 cm^{-1}
197 corresponded to C-H stretching in tween 20. A strong band at 1733 cm^{-1} attributed to C=O
198 stretching representing the carbonyl group in tween 20. Characteristic band at around 1462 cm^{-1}
199 can be related to CH_2 bending tween 20. Characteristic and sharp peak at 1091 cm^{-1} is assigned
200 to C-O stretching. FTIR of *C. aurantium* EO nanoemulsion spectrum (Figure 3C) showed the
201 broadband at 3518 cm^{-1} attributed to OH stretching vibration due to the strong hydrogen bonding
202 between water, tween 20, and phenolic and alcoholic compounds in EO. Any band at 2969,
203 2924, and 2856 cm^{-1} is related to C-H stretching due to sp^3 hybrid in tween 20 and EO. Strong
204 band at 1728 cm^{-1} showed carbonyl stretching (C=O) tween 20 and EO. The absorption at around
205 1456 cm^{-1} corresponded to CH_2 bending tween and EO. A sharp and strong peak at about 1093
206 cm^{-1} can be attributed to C-O stretching.

207 Spectrum of the *A. annua* EO has been demonstrated in Figure 3D, a broad and characteristic
208 band at about 3520 cm^{-1} , can be attributed to the hydroxyl functional groups in EO, and a band at
209 3084 cm^{-1} , allocated to the stretching vibration of =C-H groups from olefins in sp^2 hybrid. Peaks
210 at 2963, 2928, and 2872 cm^{-1} , related to stretching vibrations of -CH in sp^3 hybrid, the spectra at
211 around 1743 cm^{-1} related to C=O, the absorption around 1620 and 1415 cm^{-1} assigned to C = C,
212 the bands at 1215 and 1167 cm^{-1} are related to (C-O-C) bonds and the band at 876 cm^{-1} can be

213 allocated to angular deformations of CH₂ groups. Spectra of nanoemulsion without *A. annua* EO
214 has been shown in **Figure 3E**. A characteristic and broad peak between 3200 to 3600 cm⁻¹
215 corresponds to OH stretching vibration due to the hydrogen bonding between water and tween
216 80. Spectra at 2964 and 2925 cm⁻¹ are related to C-H stretching. Absorption at 1740 cm⁻¹ was
217 attributed to carbonyl stretching (C=O) in tween 80 and at about 1456 cm⁻¹ can be allocated to
218 CH₂ bending. A strong and characteristic band at 1080 cm⁻¹ corresponded to C-O stretching.
219 ATR-FTIR of nanoemulsion containing *A. annua* EO has been displayed in **Figure 3F**. A peak at
220 about 3422 cm⁻¹ is attributed to OH stretching vibration due to hydrogen bonding between EO,
221 tween 80, and water and at 2924 cm⁻¹ corresponds to C-H stretching of EO and tween 80.
222 Absorption at 1733 cm⁻¹ attributed to C=O stretching representing the carbonyl group in EO and
223 tween. A characteristic peak at about 1462 cm⁻¹ outlined CH₂ bending in EO and tween 80. A
224 strong and sharp peak at 1091 cm⁻¹ was assigned to C-O stretching. The presence of other bands
225 in EOs and blanks confirmed the successful loading of EOs in the prepared nanoemulsion.

226



۲۲۷

۲۲۸

۲۲۹

۲۳۰

۲۳۱

۲۳۲

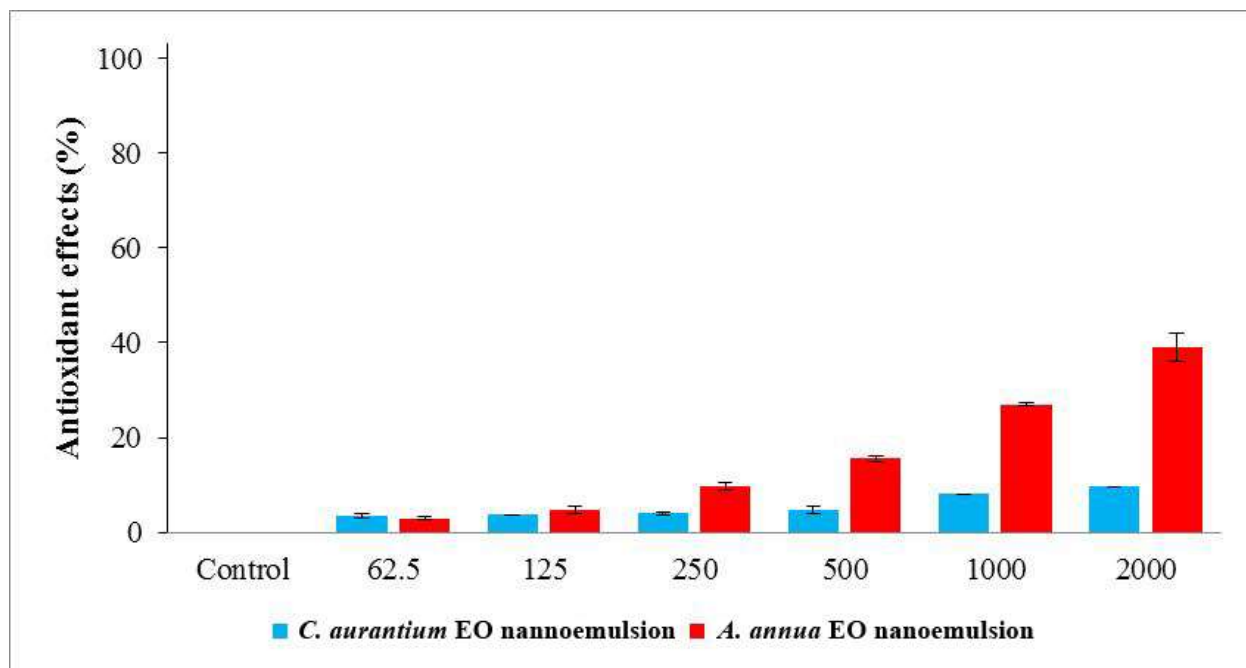
۲۳۳

۲۳۴

۲۳۵

Figure 3. ATR-FTIR spectra of A: *C. aurantium* EO, B: nanoemulsion without *C. aurantium* EO, C: nanoemulsion containing *C. aurantium* EO, D: *A. annua* EO, E: nanoemulsion without *A. annua* EO, F: nanoemulsion containing *A. annua* EO

The *C. aurantium* and *A. annua* nanoemulsions were evaluated for their antioxidant effect by DPPH assay. As shown in **Figure 4**, the most potent free radical scavenging activity was obtained from *A. annua* EO nanoemulsion, 40 % at 2000 $\mu\text{g/mL}$.



۲۳۶

۲۳۷

Figure 4. The antioxidant effects of samples

۲۳۸ **3.3. The minimum inhibitory concentration (MIC) and minimum bactericidal**
 ۲۳۹ **concentration (MBC)**

۲۴۰ From Table 3, the *C. aurantium* EO nanoemulsion MIC against *S. aureus*, *E. coli*, *P.*
 ۲۴۱ *aeruginosa*, and *K. pneumonia* included 500 µg/mL, 1000 µg/mL, 1000 µg/mL, and 1000
 ۲۴۲ µg/mL, respectively. The MBC values against bacterial strains also included >2000µg/mL.
 ۲۴۳ Moreover, The MIC values of *A. annua* nanoemulsion EO against *S. aureus*, *E. coli*, *P.*
 ۲۴۴ *aeruginosa*, and *K. pneumonia* included 1000 µg/mL, 2000 µg/mL, 2000 µg/mL, and 2000
 ۲۴۵ µg/mL, respectively. The MBC values included >2000 µg/mL for all the tested bacterial strains.

۲۴۶

Table 3. The MIC and MBC levels (µg/mL) samples

Samples	<i>S. aureus</i> (MIC, MBC)	<i>E. coli</i> (MIC, MBC)	<i>P. aeruginosa</i> (MIC, MBC)	<i>K. pneumonia</i> (MIC, MBC)
<i>C. aurantium</i> EO nanoemulsion	500, >2000	1000, >2000	1000, >2000	1000, >2000

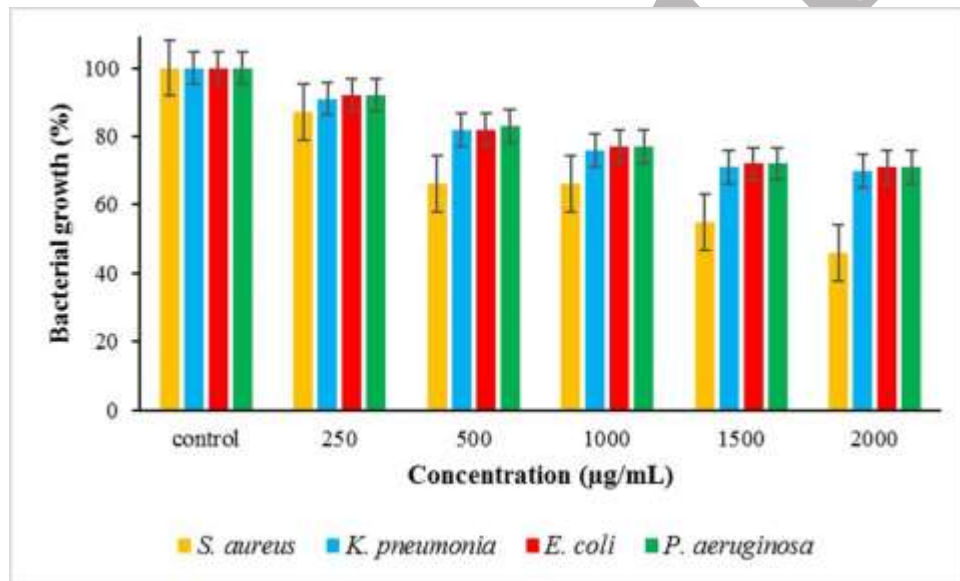
<i>A. annua</i> EO nanoemulsion	1000, >2000	2000, >2000	2000, >2000	2000, >2000
---------------------------------	-------------	-------------	-------------	-------------

247

248 3.4. Antibacterial effects

249 The bacterial growth inhibitory effect of *C. aurantium* nanoemulsion EO was
 250 concentration-dependent. The highest bactericidal effect was observed against *S. aureus* at 2000
 251 $\mu\text{g/mL}$, in which 56% of growth was inhibited (Figure 5).

252



253

254 **Figure 5.** The bacterial growth in exposure to *C. aurantium* nanoemulsion EO
 255 The growth inhibitory effect of *A. annua* nanoemulsion EO was mostly against *S. aureus*
 256 at 2000 $\mu\text{g/mL}$, at which ~20 % of bacterial growth was inhibited (Figure 6).

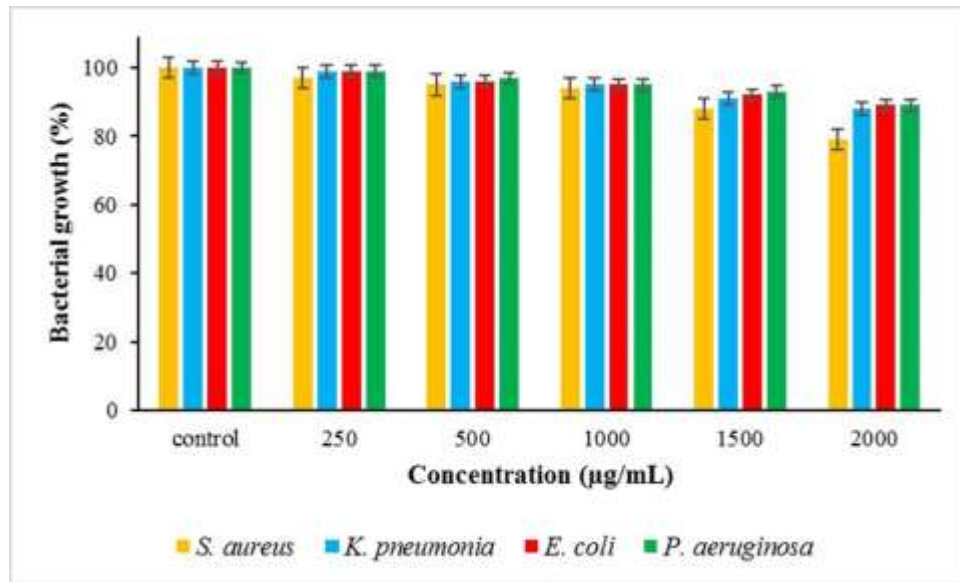


Figure 6. The bacterial growth in exposure to *A. annua* nanoemulsion EO

3.5. Anti-biofilm effects

As shown in **Figure 7**, biofilms in the control group all bacteria were formed (OD > 0.083). However, after treatment with both nanoemulsions, no biofilm (OD < 0.083) was formed by all examined bacteria, i.e., *S. aureus*, *K. pneumonia*, *E. coli*, and *P. aeruginosa*.

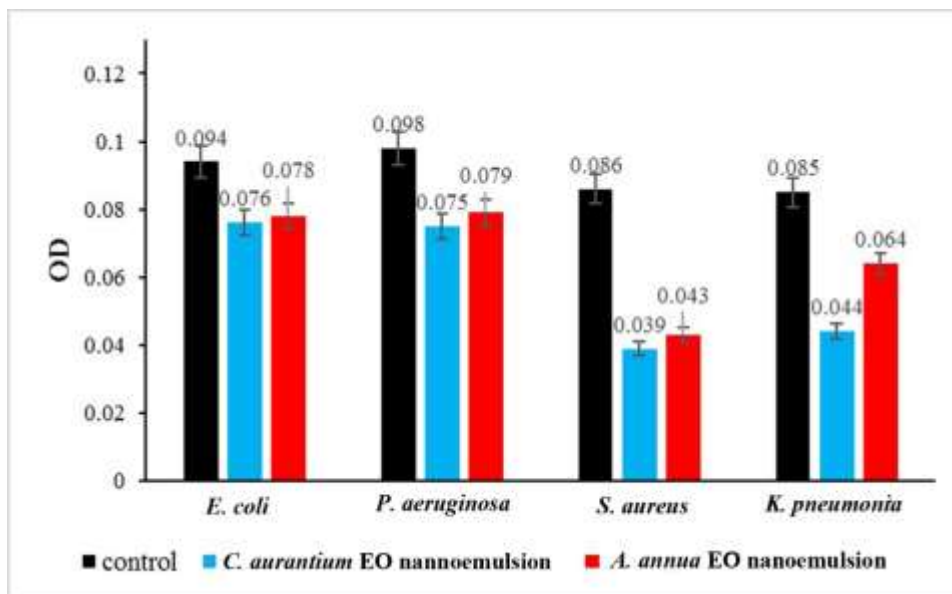


Figure 7. The anti-biofilm effects of (mean OD value) samples

4. Discussion

In our study, nanoemulsions of *C. aurantium* and *A. annua* EOs were prepared using spontaneous emulsification. Meanwhile, their antimicrobial and antibiofilm against selected bacterial pathogens were investigated. Some previous studies have investigated antimicrobial and insecticide properties of *C. aurantium* and *A. annua* extracts and EOs against different microorganisms, but our study has been carried out mostly on their nanoemulsion forms (22). For example, the biological activity and antibiofilm molecular profile of *C. aurantium* EO were investigated by Kačániová et al., that concluded that *C. aurantium* EO had potent antibacterial activity against *Stenotrophomonas maltophilia* and *Bacillus subtilis* followed by *Penicillium crustosum* (15). In addition, EOs extracted from the peel of *C. aurantium*, as noted by Madhuri et al., can be used against infectious agents such as *K. pneumoniae* and *Bacillus cereus* (23). *In vitro* studies by Marinas et al. also showed that *A. annua* EO has selective antipathogenic activity on Gram-positive and Gram-negative bacterial strains (24). Its antibacterial and anti-biofilm activities have been also unveiled (25, 26). In addition, Mariadosset et al. fabricated the selenium

281 nanoparticles using *A. annua* (AaSeNPs) of 109.2 nm in size and the characterized AaSeNPs
282 indicated an antibacterial activity against multidrug-resistant pathogens such as *S. aureus*, *B.*
283 *subtilis*, *Proteus mirabilis*, and *E. coli* (27). As well as the results obtained by Das et al. showed
284 stronger antimicrobial activity of Pickering nanoemulsion of the *Artemisia* essential oil (26). In
285 our study, antimicrobial and antibiofilm effects of nanoemulsions of *C. aurantium* and *A. annua*
286 EOs against selected bacterial pathogens were confirmed by MIC and MBC tests with the
287 highest activity against *S. aureus*. Exposure of pathogens with nanoemulsions resulted in a
288 significant reduction in the biofilm formation by all examined bacteria i.e., *S. aureus*, *K.*
289 *pneumonia*, *E. coli*, and *P. aeruginosa*. This study firstly investigated the chemical composition
290 of *C. aurantium* and *A. annua* EO. Their nanoemulsion dosage forms were then prepared. The
291 antimicrobial and antibiofilm activities of nanomulsions were unraveled. Both nanoemulsions
292 inhibited the growth of *S. aureus*. Interestingly, no biofilms of *S. aureus*, *K. pneumonia*, *E. coli*,
293 and *P. aeruginosa* were observed after treatment with these nanoemulsions. Moreover, *A. annua*
294 nanoemulsion inferred potent antioxidant properties. Limitations of this study mostly included
295 low number of bacterial pathogens, lack of *in silico* assessment of binding of bioactive
296 compounds to bacterial targets and lack of *in vivo* study.

297 **Acknowledgements**

298 This study was supported by Fasa University of Medical Sciences.

299 **Authors' contributions**

300 MO and AG conceptualized and designed the study. AG performed antibacterial tests and
301 revised the MS. HA drafted MS in cooperation with MO. MAH and BM prepared
302 nanoemulsions. EZ interpreted ATR-FTIR. MZ performed the DPPH assay. MO designed the

۳۰۳ study, supervised the project, and drafted the MS. All authors contributed to drafting MS and
۳۰۴ approved the final version.

۳۰۵ **Conflict of interest**

۳۰۶ None to declare.

۳۰۷ **Data availability**

۳۰۸ The data used to support the findings of this study are available from the corresponding author
۳۰۹ upon request.

۳۱۰ **Funding**

۳۱۱ Fasa University of Medical Sciences supported this study supported the study.

۳۱۲ **Ethics**

۳۱۳ Fasa University of Medical Sciences supported this study, grant No. 401268. Besides, it was
۳۱۴ ethically approved; IR.FUMS.REC.1401.205.

۳۱۵ **Reference**

- ۳۱۶ 1. Mestrovic T, Aguilar GR, Swetschinski LR, Ikuta KS, Gray AP, Weaver ND, et al. The burden of
۳۱۷ bacterial antimicrobial resistance in the WHO European region in 2019: A cross-country systematic
۳۱۸ analysis. *The Lancet Public Health*. 2022;7(11):e897-e913.
- ۳۱۹ 2. Laxminarayan R. The overlooked pandemic of antimicrobial resistance. *The Lancet*.
۳۲۰ 2022;399(10325):606-7.
- ۳۲۱ 3. Noorpisheh Ghadimi S, Sharifi N, Osanloo M. The leishmanicidal activity of essential oils: A
۳۲۲ systematic review. *Journal of Herbmmed Pharmacology*. 2020;9(4):300-8.
- ۳۲۳ 4. Qasemi H, Fereidouni Z, Karimi J, Abdollahi A, Zarenezhad E, Rasti F, et al. Promising
۳۲۴ antibacterial effect of impregnated nanofiber mats with a green nanogel against clinical and standard
۳۲۵ strains of *Pseudomonas aeruginosa* and *Staphylococcus aureus*. *Journal of Drug Delivery Science and*
۳۲۶ *Technology*. 2021:102844.
- ۳۲۷ 5. Kanwar R, Rathee J, Salunke DB, Mehta SK. Green nanotechnology-driven drug delivery
۳۲۸ assemblies. *ACS omega*. 2019;4(5):8804-15.
- ۳۲۹ 6. Swain SS, Paidesetty SK, Padhy RN, Hussain T. Nano-technology platforms to increase the
۳۳۰ antibacterial drug suitability of essential oils: A drug prospective assessment. *OpenNano*. 2022:100115.
- ۳۳۱ 7. Rahchamani R, Zarooni S, Borhani MS. The Chemical Composition and Antibacterial Effect of
۳۳۲ Essential Oils of Rosemary and Basil in Milk. *Iranian Journal of Veterinary Medicine*. 2024.
۳۳۳ DOI:10.22059/IJVM.2024.3 2443 7 .100 7 5 51.
- ۳۳۴ 8. Farzaneh M, Fadaei V, Gandomi H. Antioxidant, Syneresis, and Sensory Characteristics of
۳۳۵ Probiotic Yogurt Incorporated With Agave tequilana Aqueous Extract. *Iranian Journal of Veterinary*
۳۳۶ *Medicine*. 2023;17(3):243-52.

- 337 9. Ali Anvar SA, Nowruzi B, Afshari G. A Review of the Application of Nanoparticles Biosynthesized
 338 by Microalgae and Cyanobacteria in Medical and Veterinary Sciences. *Iranian Journal of Veterinary*
 339 *Medicine*. 2023;17(1).
- 340 10. Khaji L, Noori N, Jebelli Javan A, Khanjari A, Ghandomi Nasrabadi H. Antimicrobial effect of
 341 *Cuminum Cyminum* essential oil on Iranian white soft cheese in air and modified atmosphere packaging
 342 during refrigerated storage. *Iranian Journal of Veterinary Medicine*. 2023.
- 343 11. Maksoud S, Abdel-Massih RM, Rajha HN, Louka N, Chemat F, Barba FJ, et al. *Citrus aurantium* L.
 344 Active Constituents, Biological Effects and Extraction Methods. An Updated Review. *Molecules*.
 345 2021;26(19).
- 346 12. Gao L, Zhang H, Yuan CH, Zeng LH, Xiang Z, Song JF, et al. *Citrus aurantium* 'Changshan-huyou'-
 347 An ethnopharmacological and phytochemical review. *Frontiers in Pharmacology*. 2022;13:983470.
- 348 13. Liu S, Lou Y, Li Y, Zhang J, Li P, Yang B, et al. Review of phytochemical and nutritional
 349 characteristics and food applications of *Citrus* L. fruits. *Frontiers in Nutrition*. 2022;9:968604.
- 350 14. Okla MK, Alamri SA, Salem MZ, Ali HM, Behiry SI, Nasser RA, et al. Yield, phytochemical
 351 constituents, and antibacterial activity of essential oils from the leaves/twigs, branches, branch wood,
 352 and branch bark of Sour Orange (*Citrus aurantium* L.). *Processes*. 2019;7(6):363.
- 353 15. Kačaniová M, Terentjeva M, Galovičová L, Ivanišová E, Štefániková J, Valková V, et al. Biological
 354 activity and antibiofilm molecular profile of *Citrus aurantium* essential oil and its application in a food
 355 model. *Molecules*. 2020;25(17):3956.
- 356 16. Anibogwu R, Jesus K, Pradhan S, Pashikanti S, Mateen S, Sharma K. Extraction, Isolation and
 357 Characterization of Bioactive Compounds from *Artemisia* and Their Biological Significance: A Review.
 358 *Molecules*. 2021;26(22).
- 359 17. Bilia AR, Santomauro F, Sacco C, Bergonzi MC, Donato R. Essential Oil of *Artemisia annua* L.: An
 360 Extraordinary Component with Numerous Antimicrobial Properties. *Evidence Based Complementary and*
 361 *Alternative Medicine*. 2014;2014:159819.
- 362 18. Mirzaei-Najafgholi H, Tarighi S, Golmohammadi M, Taheri P. The Effect of *Citrus* Essential Oils
 363 and Their Constituents on Growth of *Xanthomonas citri* subsp. *citri*. *Molecules*. 2017;22(4):591.
- 364 19. Osanloo M, Ghaznavi G, Abdollahi A. Sureveying the chemical composition and antibacterial
 365 activity of essential oils from selected medicinal plants against human pathogens. *Iranian Journal of*
 366 *Microbiology*. 2020;12(6):505-12.
- 367 20. Catania AM, Di Ciccio P, Ferrocino I, Civera T, Cannizzo FT, Dalmasso A. Evaluation of the biofilm-
 368 forming ability and molecular characterization of dairy *Bacillus* spp. isolates. *Frontiers in Cellular and*
 369 *Infection Microbiology*. 2023;13.
- 370 21. Stepanovic S, Vukovic D, Dakic I, Savic B, Svabic-Vlahovic M. A modified microtiter-plate test for
 371 quantification of staphylococcal biofilm formation. *Journal of Microbiological Methods*. 2000;40(2):175-
 372 9.
- 373 22. Durán Aguirre CE, Pratisoli D, Damascena AP, Romário de Carvalho J, de Araujo Junior LM.
 374 Lethal and sublethal effects of *Citrus aurantium* and *Citrus sinensis* essential oils and their major
 375 component limonene on *Helicoverpa armigera* (Hübner) (Lepidoptera: Noctuidae). *Journal of Essential*
 376 *Oil Bearing Plants*. 2024;27(3):838-48.
- 377 23. Madhuri S, Hegde AU, Srilakshmi N, Prashith Kekuda T. Antimicrobial activity of *Citrus sinensis*
 378 and *Citrus aurantium* peel extracts. *Journal of Pharmaceutical and Scientific Innovation (JPSI)*.
 379 2014;3(4):366-8.
- 380 24. Marinas IC, Oprea E, Chifiriuc MC, Badea IA, Buleandra M, Lazar V. Chemical composition and
 381 antipathogenic activity of *Artemisia annua* essential oil from Romania. *Chemistry & Biodiversity*.
 382 2015;12(10):1554-64.

25. Al-Mothafar NA, Al-Shahwany AW. Phenolic compounds from *Thymus vulgaris*, *Artemisia annua* extracts and pure Thymol were tested against twenty *Pseudomonas* spp. strains for antibacterial and anti-biofilm activities. IOP Journal of Physics Under review. 2022
26. Das S, Vörös-Horváth B, Bencsik T, Micalizzi G, Mondello L, Horváth G, et al. Antimicrobial activity of different *Artemisia* essential oil formulations. *Molecules*. 2020;25(10):2390.
27. Mariadoss AVA, Saravanakumar K, Sathiyaseelan A, Naveen KV, Wang M-H. Enhancement of anti-bacterial potential of green synthesized selenium nanoparticles by starch encapsulation. *Microbial Pathogenesis*. 2022;167:105544.

391

Preprint